

# POLAR magnetic field observations at apogee during the January 1997 magnetic cloud event

F. R. Fenrich, J. G. Luhmann

Space Sciences Laboratory, University of California, Berkeley

G. Le, C. T. Russell

Institute of Geophysics and Planetary Physics, University of California, Los Angeles

**Abstract.** Magnetic field measurements from the POLAR satellite are presented for three dusk to dawn apogee passes during the January 1997 magnetic cloud event. The variability in the residual fields from one orbit to the next are investigated in terms of the changing solar wind and magnetospheric current systems. The observed fields are compared to the Tsyganenko 96 (T96\_01) model which allows dynamic solar wind and Dst inputs. The model fields are found to generally agree with the observed fields with the greatest discrepancy occurring during periods of large dynamic pressure. An investigation of the contributions to the T96\_01 model by the various solar wind and Dst inputs provides insight into the solar wind control of the high altitude magnetosphere above the polar cap. It is found that the ring current is responsible for the largest proportion of the observed magnetic field residuals while the interplanetary magnetic field and solar wind dynamic pressure control a smaller proportion primarily producing the shorter time scale variations in the observed fields.

## Introduction

The impact of a magnetic cloud with the Earth such as the January 1997 event provides an ideal opportunity for the study of the coupling between solar wind and magnetosphere. Of particular interest in this paper is the effect of the varying solar wind conditions on the high latitude, high altitude magnetosphere, as determined by the magnetic fields experiment (MFE) on POLAR [Russell *et al.*, 1995]. By comparing the observed fields during successive apogee passes, each characterized by significantly different solar wind conditions, we can gain insight into how the high altitude magnetosphere responds to those different conditions. The T96\_01 model is used as a tool to determine which solar wind and Dst parameters are most likely responsible for the observed magnetic field variations. The T96\_01 model is controlled by the solar wind dynamic pressure ( $P_{dyn}$ ), interplanetary magnetic fields (IMF  $B_y$  and  $B_z$ ), and the Dst index [Tsyganenko, 1995, 1996; Tsyganenko and Stern, 1996].

The solar wind and Dst parameters during the January 1997 magnetic cloud event are presented in Figure 1. The three intervals to be investigated are highlighted and include a wide range of solar wind conditions which should produce

markedly different magnetospheric responses. The POLAR Magnetic Fields Experiment monitors these responses along the satellite's trajectory as it passes through the high altitude near-terminator magnetosphere. An investigation of the POLAR MFE fields at perigee during the Jan 1997 event reported in a companion paper [Le *et al.*, 1998] illustrates the different sensitivity at low altitudes to the passage of magnetic clouds.

## Observations and Model Results

The POLAR spacecraft is in a high inclination orbit with an apogee of 9 Re over the north pole, a perigee of 1.8 Re, and a period of 17.5 hours. As an example the orbital trajectory for the Jan 10 interval is shown in Figure 2. Similarly, the trajectories corresponding to the other two intervals also lie close to the dusk-dawn plane above the north pole, beginning at dusk and ending at dawn. The observed MFE fields for all three intervals are shown in Figure 3 together with the T96\_01 model fields. All observed fields are the residual fields from the International Geomagnetic Reference Field at epoch of date (IGRF 95 model) while the T96\_01 fields include only the external model fields determined using the observed solar wind and Dst parameters as input. The model is correctly predicting the observations when the dotted line overlays the solid line.

As expected there are some significant differences between the three time periods as a result of the different solar wind conditions. However, there are also some general trends which are consistent from one apogee pass to the next. For example, the  $B_x$  and total B field residuals are consistently positive, the  $B_y$  residual reverses across the polar cap, and the  $B_z$  residual is consistently negative. For the most part there is good agreement with the T96\_01 model on each of these days. The greatest disagreements with the model occur during periods of the most extreme solar wind conditions. In the following section we discuss which current systems and solar wind inputs contribute to these magnetic field residuals.

## Discussion

The separate contributions to the T96\_01 model fields by the different solar wind dynamic inputs are plotted in Figure 4. Figure 4a shows the model field contributions due to the ring current while Figure 4b is plotted with a smaller vertical scale to emphasize the model field contributions from the solar wind dynamic pressure (dotted line) and the interplanetary magnetic field (solid line). These figures allow

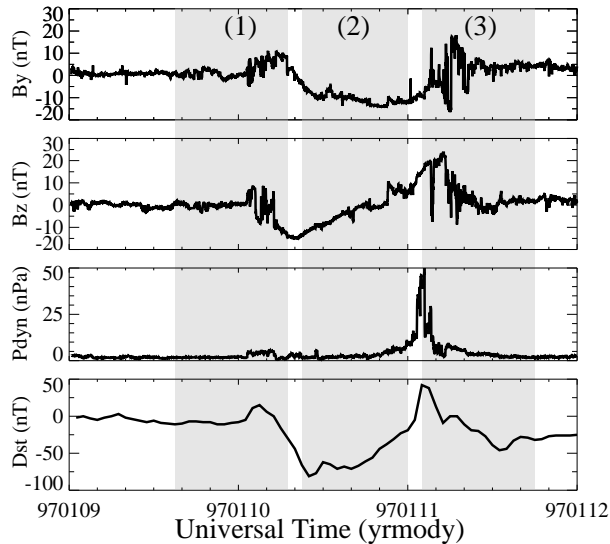


**Figure 1.** The solar wind and Dst parameters during the January 9–11, 1997 magnetic cloud event with the three time intervals of interest highlighted. Note that the timing of the solar wind data acquired from the WIND satellite has been adjusted to correspond to the time at which the solar wind flow reaches the Earth. Dst is the preliminary Dst index measured by WDC-C2 for Geomagnetism, Kyoto.

us to examine which solar wind inputs to the T96.01 model contribute the most to the model external magnetic fields. Given the good agreement between the T96.01 model and the POLAR MFE fields the assumption is made that the solar wind parameters also contribute to the observed magnetic field residuals in a similar manner.

### Effect of Ring Current

Upon comparing Figures 4a and 4b and taking note of the smaller vertical scale in Figure 4b, it is apparent that the ring current is responsible for most of the  $B_y$ ,  $B_z$  and total B field residuals in all three time intervals. During each interval the ring current contribution is greatest near the equatorial plane where it produces the large negative  $B_z$  and total B field depression. The most pronounced ring current contributions occur during the Jan 10 interval when the Dst index is most negative (see Figure 1).

Referring back to Figure 3 the largest differences between the observed and model fields occur near the equatorial

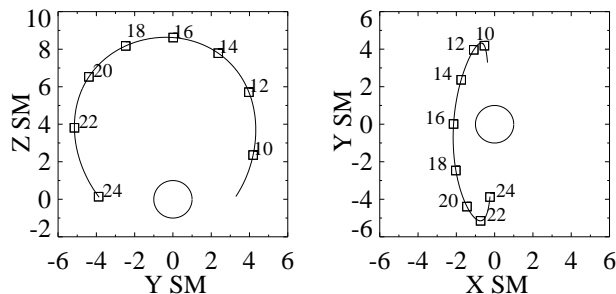


**Figure 2.** POLAR satellite trajectory during the January 10 apogee pass. The trajectory is plotted in SM coordinates.

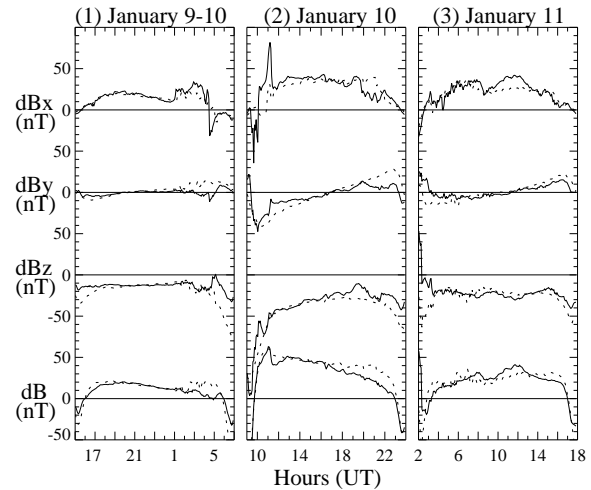


**Figure 3.** POLAR MFE residuals from IGRF (solid line) and external T96.01 fields with dynamic solar wind inputs (dotted line) for each of the three time intervals of interest. All fields are plotted in SM coordinates.

plane where the ring current fields dominate. One example of this occurs from 0600–0700 UT at the end of the January 9–10 pass as POLAR approaches the dawn equatorial plane. During this time the T96.01 model overestimates the negative  $B_z$  residual by as much as 50 nT. This discrepancy is attributed to an asymmetric ring current for the following reason. Just a few hours later on Jan 10 between 0900 and 1000 UT when POLAR is passing through the dusk equatorial plane the T96.01 model slightly underestimates the negative  $B_z$  residual even though the solar wind conditions are quite similar to the earlier 0600–0700 UT time interval (see Figure 1). Since the T96.01 model does not incorporate an asymmetric ring current the existence of such an asymmetry with a stronger ring current at dusk and a weaker ring current at dawn would produce the observed discrepancies. A similar asymmetry is also seen at low altitudes [Le *et al.*, 1998].

However, not all periods of large discrepancy can be attributed to ring current effects. Some of the largest differences between model and measured fields occur during periods of enhanced dynamic pressure and variable IMF such as at the end of the Jan 10 interval and the beginning of the Jan 11 interval. In such cases many factors contribute to the overall discrepancy between the model and measured magnetic fields.

### Effect of IMF Variability

As shown by the solid line in Figure 4b, the IMF is responsible for much of the short time variation in the model magnetic field residuals as well as some of the longer lasting trends such as positive  $dB_x$  and negative  $dB_z$  on Jan 10. In the T96.01 model the IMF inputs affect both tail and field aligned currents as well as the interconnection fields in the boundary layer. Thus in the observed MFE residuals in Figure 3 a good portion of the short time variability is most likely due to tail and field aligned currents controlled by the changing IMF.

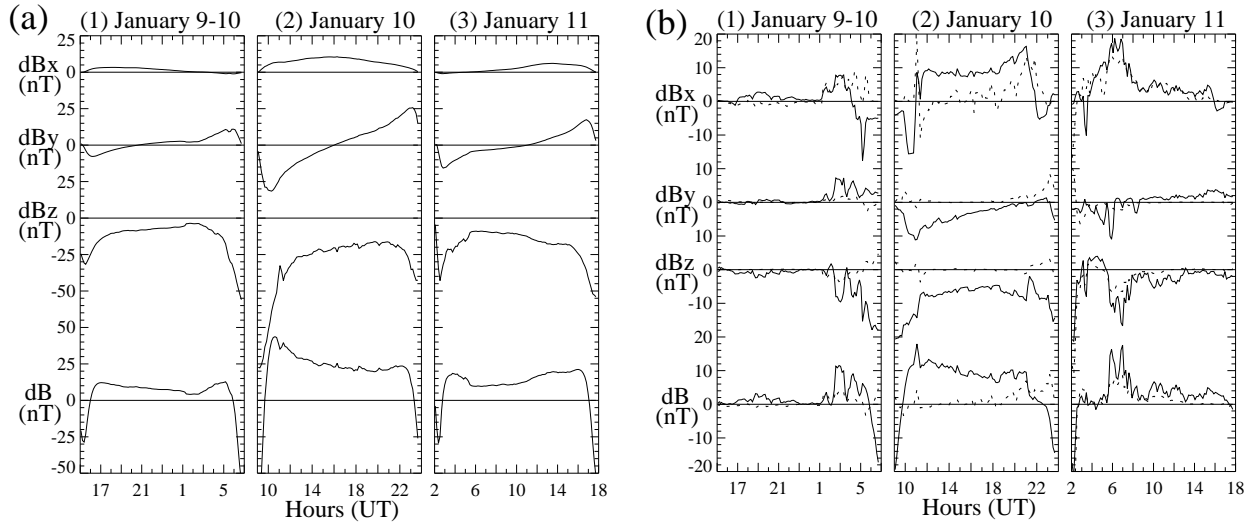


**Figure 4.** Individual contributions to the T96.01 external fields along the POLAR satellite trajectories from (a) the ring current, and (b) the variable solar wind dynamic pressure (dotted line) and variable IMF (solid line). The fields are plotted in SM coordinates and the vertical scale is smaller in 4b.

**Effect of Solar Wind Dynamic Pressure**

In Figure 4b, the dotted line represents the model field contributions from just the solar wind dynamic pressure variations. The contributions are primarily in the x direction and result from an increase in magnetopause currents as well as tail and field aligned currents associated with the changes in dynamic pressure.

One of the most interesting features is the narrow positive peak in the contribution to dBx at 1100 UT on Jan 10. In Figure 3 this peak is seen very strongly in the measured dBx field and to a lesser extent in the model dBx field. Comparing this time interval to the solar wind parameters in Figure 1 it is apparent that this feature is indeed due to a small sharp impulse in dynamic pressure at approximately the same time. The response of the T96.01 model to this pressure pulse greatly underestimates the actual response. In fact during all periods of strong dynamic pressure the model has difficulty reproducing the measured fields.

There are other significant enhancements in dynamic pressure, for example between 0200 and 0400 UT on Jan 11, which do not produce nearly as great an effect as the 1100 UT Jan 10 pressure pulse. These relatively weaker responses to dynamic pressure may be due to the fact that the IMF is not strongly southward as it is on Jan 10 implying that the solar wind dynamic pressure may have a much larger effect during periods of southward IMF. In support of this is the simultaneous peak in the model field contributions from both *P<sub>dyn</sub>* and IMF on Jan 10 near 1100 UT as seen in Figure 4b.

**Field Aligned Currents**

Using a field aligned coordinate system Figure 5 plots the observed MFE residuals together with those contributions to the T96.01 model fields from field aligned currents only. Note that the field aligned coordinate system is based upon the T96.01 fields with input parameters *P<sub>dyn</sub>* = 2.0 nPa, *Dst* = 0, IMF *B<sub>y</sub>* = IMF *B<sub>z</sub>* = 0, and with IGRF 95 as the internal field. The z-direction is along the local model

magnetic field, y is perpendicular to the model field and eastward and x completes the right-handed system. In such a coordinate system field aligned current signatures will be most pronounced in the y-direction. It is found that field aligned currents contribute only a small amount to the total model external fields. However, there are a couple of large features in the observed MFE residuals that appear to be due to field aligned currents. The sharp changes in dBy between 0400 and 0500 UT and between 0900 and 1000 UT on Jan 10 are both consistent with the POLAR satellite passing through the Birkeland field aligned current system. Near these times the T96.01 model predicts some field

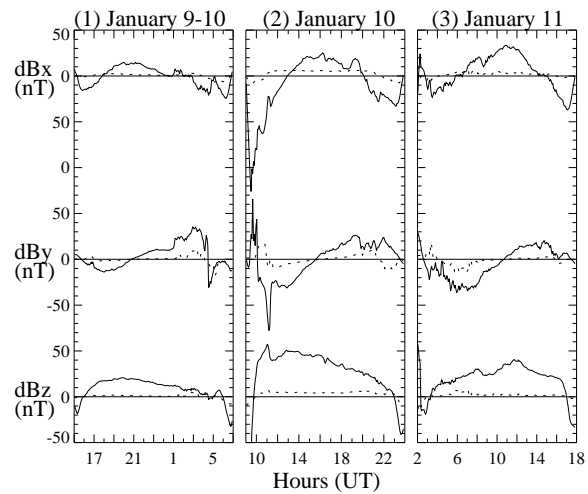


**Figure 5.** POLAR MFE residuals from the IGRF (solid line) and external T96.01 field contribution from field aligned currents only (dotted line). The fields are plotted in a field aligned coordinate system that is based upon a steady-state quiet time T96.01 model with internal IGRF fields.

aligned current effects but they are significantly weaker and are delayed by approximately one hour from the observed signatures.

These field aligned current signatures seen at apogee differ from those seen at perigee on Jan 10 [Le *et al.*, 1998] in that they are almost an order of magnitude smaller and they do not dominate the residual field pattern as they do throughout the perigee pass on this day.

## Conclusions

The MFE residual fields during three successive apogee passes of the POLAR satellite exhibit distinctive features superimposed upon similar general trends. The similar trends which, in SM coordinates, include positive dBx and dB, negative dBz, and a reversal of dBy, are a result of quiet time magnetopause, tail and ring currents. The distinctive features are attributed to the variable solar wind and Dst parameters. The ring current has a large effect on both the inner and outer magnetosphere during the magnetic cloud passage being responsible for most of the observed By, Bz and total B residuals along all three apogee passes. The effect of the ring current is greatest in the near equatorial regions during the Jan 10 interval when the IMF is southward. There is also evidence for a dawn-dusk asymmetry in the ring current strength during the main phase of the Jan 10 magnetic storm. The solar wind dynamic pressure and IMF variability are responsible for the shorter time scale variations with the dynamic pressure having greater effect during periods of southward IMF. There are two instances where field aligned current effects are seen. Both of these instances are during the southward IMF portion of the magnetic cloud and are seen at the lower altitude portion of the apogee trajectories at radial distances of  $\sim 4$ -6 RE.

The response of the magnetosphere to the passage of the magnetic cloud is modeled very effectively by the T96.01 model. The model has proved to be a very useful tool in

determining the solar wind control of the magnetic fields at high altitudes above the north pole.

**Acknowledgments.** This research was supported by the National Aeronautics and Space Administration under research grant NAG5-3171. F.R. Fenrich thanks the Natural Sciences and Engineering Research Council of Canada for their support. The authors also thank K. Ogilvie for the Solar Wind Experiment key parameters, R. Lepping for the WIND Magnetic Fields Investigation key parameters, and WDC-C2 Kyoto for the provisional Dst measurements.

## References

- Le, G., C. T. Russell, and J. G. Luhmann, POLAR magnetic observations of the low-altitude magnetosphere during the January 1997 coronal mass ejections/magnetic cloud event, *Geophys. Res. Lett.*, in press, 1998.
- Russell, C. T., R. C. Snare, J. D. Means, D. Pierce, D. Dearborn, M. Larson, G. Barr, G. Le, The GGS/POLAR magnetic fields investigation, *Space Sci. Rev.*, *71*, 563-582, 1995.
- Tsyganenko, N. A., Modeling the Earth's magnetospheric magnetic field confined within a realistic magnetopause, *J. Geophys. Res.*, *100*, 5599-5612, 1995.
- Tsyganenko, N. A., Effects of the solar wind conditions on the global magnetospheric configuration as deduced from data-based field models, *Proceedings of the ICS-3 Conference on substorms* (Versailles, France, May 12-17, 1996), *ESA SP-389*, 81-185, 1996.
- Tsyganenko, N. A., D. P. Stern, Modeling the global magnetic field of the large-scale Birkeland current systems, *J. Geophys. Res.*, *101*, 27187-27198, 1996.

---

F. R. Fenrich, J. G. Luhmann, Space Sciences Laboratory, University of California, Berkeley, CA 94720. (e-mail: ffenrich@ssl.berkeley.edu; jgluhman@ssl.berkeley.edu)

G. Le, C. T. Russell, Institute of Geophysics and Planetary Physics, University of California, Los Angeles, CA 90024. (e-mail: guan@igpp.ucla.edu; ctrussel@igpp.ucla.edu)

(Received October 15, 1997; accepted March 3, 1998.)